Eur. Phys. J. A **24**, 249–257 (2005)
DOI 10.1140/epja/i2004-10145-2

THE EUROPEAN PHYSICAL JOURNAL A

High-spin isomer in ^{93}Mo

T. Fukuchi[1,a], Y. Gono[2], A. Odahara[3], S. Tanaka[4], M. Inoue[4], Y. Wakabayashi[4], T. Sasaki[4], M. Kibe[4], N. Hokoiwa[4], T. Shinozuka[5], M. Fujita[5], A. Yamazaki[5], T. Sonoda[5], C.S. Lee[6], Y.K. Kwon[6], J.Y. Moon[6], and J.H. Lee[6]

[1] Center for Nuclear Study, University of Tokyo, Hirosawa 2-1, Wako, Saitama 351-0198, Japan
[2] Cyclotron Center, RIKEN, Hirosawa 2-1, Wako, Saitama 351-0198, Japan
[3] Nishinippon Institute of Technology, Kanda, Fukuoka 800-0361, Japan
[4] Department of Physics, Kyushu University, Hakozaki 6-10-1, Fukuoka 812-8581, Japan
[5] Cyclotron and Radioisotope Center, Tohoku University, Sendai, 980-8578, Japan
[6] Department of Physics, Chung-Ang University, Seoul 156-756, Korea

Received: 6 May 2004 / Revised version: 1 March 2005 /
Published online: 12 April 2005 –
Communicated by C. Signorini

Abstract. The high-spin states of ^{93}Mo have been studied by a ^{82}Se(^{16}O, 5n)^{93}Mo reaction at a beam energy of 100 MeV using techniques of in-beam γ-ray spectroscopy. Measurements of γ-t, γ-γ-t coincidences, γ-ray angular distributions and γ-ray linear polarizations were performed. The high-spin isomer was found as a $(39/2^-)$ state at about 9.7 MeV. The near-yrast states in ^{93}Mo were interpreted using the weak-coupling picture of a $d_{5/2}$ neutron to a neutron magic core nucleus ^{92}Mo.

PACS. 27.60.+j $90 \leq A \leq 149$

1 Introduction

High-spin isomers were reported in $N = 83$ isotones, systematically, ^{143}Nd [1], ^{144}Pm [2], ^{145}Sm [3], ^{146}Eu [4], ^{147}Gd [5], ^{148}Tb [6], ^{149}Dy [7], ^{150}Ho [8] and ^{151}Er [9]. Their lifetimes range from 10 ns to μs. The excitation energies of high-spin isomers in $N = 83$ isotones are close to each other in a range of 8.5–9.0 MeV and their spins and parities are $49/2^+$ and 27^+ for odd and odd-odd nuclei, respectively, except for ^{150}Ho and ^{151}Er. The decay scheme and the characteristics of the high-spin isomer in ^{147}Gd were studied in detail experimentally [5] and theoretically [10]. This high-spin isomer has been known to be the $49/2^+$ state at 8.6 MeV and has a 510 ns half-life [5]. The deformation parameter β of this state was determined to be -0.19 based on the measurements of the static quadrupole moment [11]. The configuration of this isomer was taken to be $[\nu(f_{7/2}h_{9/2}i_{13/2}) \otimes \pi(h^2_{11/2})]_{49/2^+}$ using the g-factor obtained experimentally [12]. According to the deformed independent particle model (DIPM) calculations [10] the nuclear shapes suddenly change from near spherical into oblate shapes at high-spin isomeric states. In a high-spin region of these nuclei, the angular momenta of individual valence particles align to the symmetry axis so that the overlaps of nucleon wave functions become maximum. This sudden shape change causes the high-spin isomer.

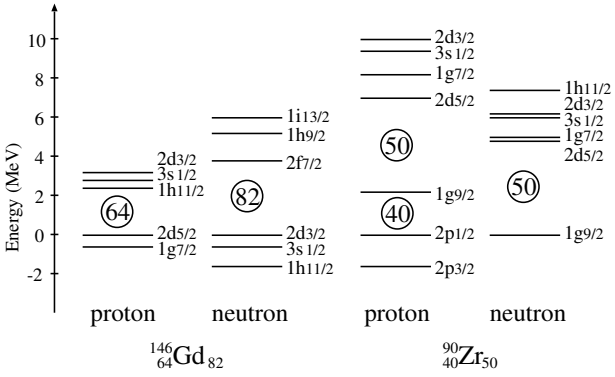

Fig. 1. Single-particle levels in the ^{146}Gd region (left side) and in the ^{90}Zr region(right side). The single-particle energies are given with respect to an arbitrary zero point.

In order to study the existence of the same kind of isomers in other mass regions, spherical single-particle orbits near Fermi levels were compared between those in mass-150 region and in mass-90 region. In the case of $N = 83$ isotones, the neutron number is the magic number 82 plus one and proton numbers are near 64 sub-shell closure. In $N = 51$ isotones, the neutron number is the magic number 50 plus one and proton numbers are near 40 sub-shell

[a] e-mail: fukuchi@cns.s.u-tokyo.ac.jp

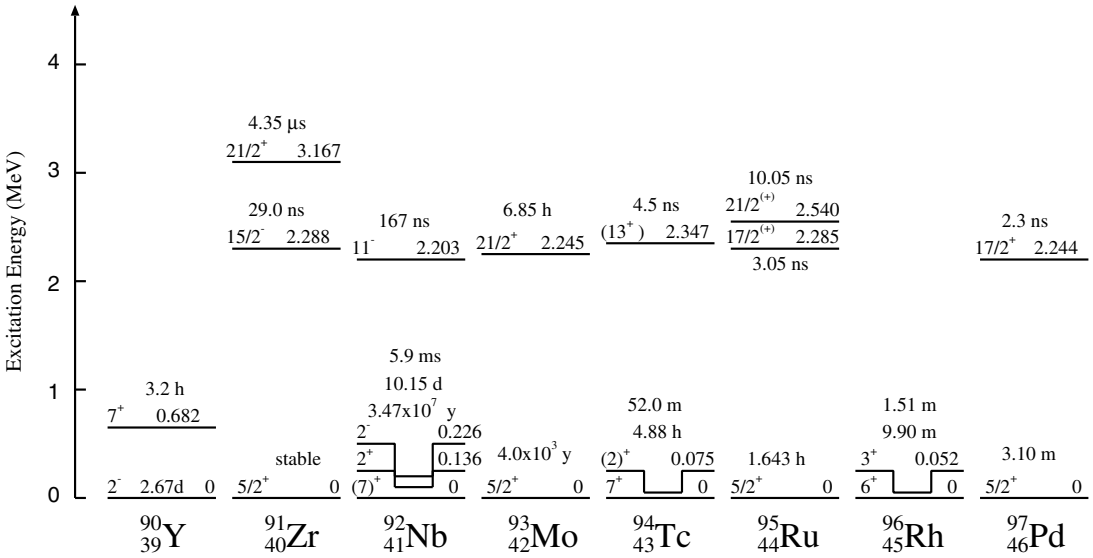

Fig. 2. Experimental systematics of isomers in $N = 51$ isotones.

closure. Figure 1 shows empirically deduced spherical single-particle levels in the ^{146}Gd [10] region and spherical single-particle energies in the ^{90}Zr region calculated using the Woods-Saxon potential.

In $N = 83$ isotones, low-spin isomers of $27/2^-$ were known for odd nuclei. A configuration of these isomers was $[\nu(f_{7/2}) \otimes \pi(h^2_{11/2})]_{27/2^-}$. On the other hand, in $N = 51$ isotones, $21/2^+$ isomers were reported. Experimental systematics of isomers in ^{90}Y [13], ^{91}Zr [14], ^{92}Nb [15], ^{93}Mo [16], ^{94}Tc [17], ^{95}Ru [18], ^{96}Rh [19], and ^{97}Pd [19] are shown in fig. 2. These isomers have $[\nu(d_{5/2})\otimes\pi(g^2_{9/2})]_{21/2^+}$ configurations in odd nuclei. Both are of the stretch coupled configurations with proton core excitations. These isomers which have the same excitation mechanism in both isotones suggest the existence of the high-spin isomer in $N = 51$ isotones. Based on the analogy of configurations of isomers in $N = 83$ and $N = 51$ isotones, the expected configurations of high-spin isomers in $N = 51$ isotones are $[\nu(d_{5/2}g_{7/2}h_{11/2})\otimes\pi(g^2_{9/2})]_{39/2^-}$ for odd nuclei, and $[\nu(d_{5/2}g_{7/2}h_{11/2})\otimes\pi(g^2_{9/2}p^{-1}_{1/2})]_{20^+}$ for odd-odd nuclei.

In this work, a member of the $N = 51$ isotones ^{93}Mo as well as its neighboring nuclei were studied using γ-ray spectroscopic methods.

2 Experimental procedure and results

Experiments to search for the high-spin isomer in ^{93}Mo were performed at Cyclotron and Radioisotope Center (CYRIC) at Tohoku University. States in ^{93}Mo were populated using the reaction ^{82}Se(^{16}O, 5n)^{93}Mo. The ^{82}Se target of 5.2 mg/cm^2 was enriched to 90% and a target foil was backed by 500 μg/cm^2 of gold for a mechanical support. The target was thick enough to stop the reaction products in it. The pulsed ^{16}O beam of 100 MeV with a repetition time of 83 ns and pulse width of less than

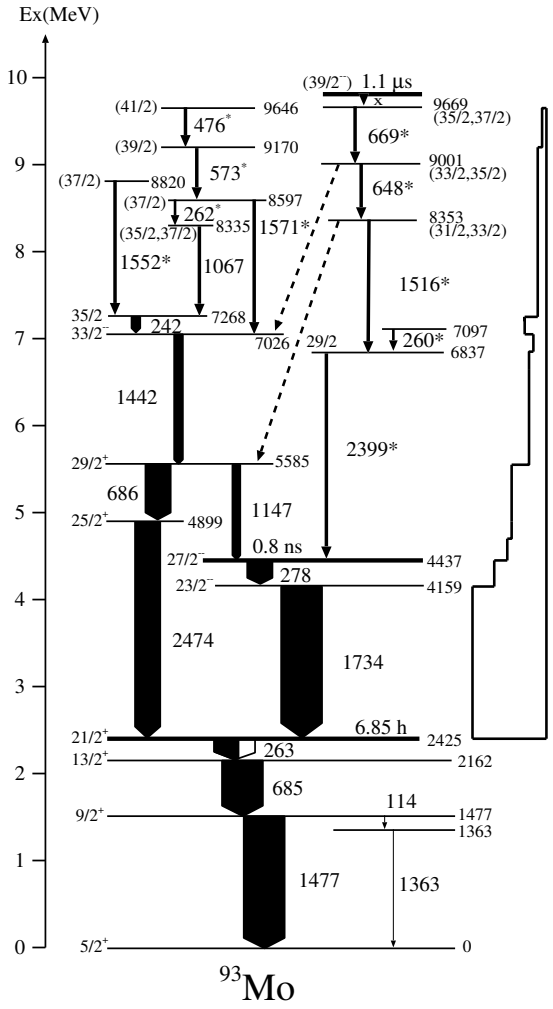

Fig. 3. The proposed level scheme for ^{93}Mo. The width of the arrows indicates γ-ray intensities, while the energies are given in keV units. The transitions marked by an asterisk are new ones.

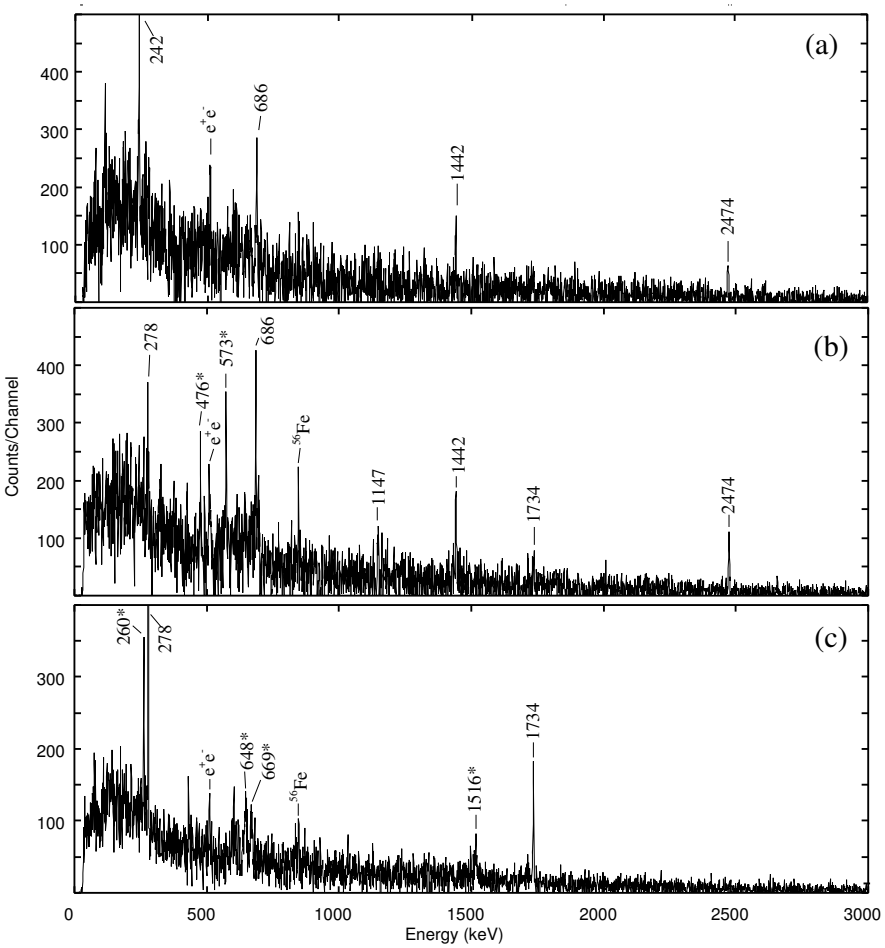

Fig. 4. Spectra obtained by gating on 1067 keV (a), 1571 keV (b) and 2399 keV (c) γ-rays.

2 ns was provided by the AVF cyclotron at CYRIC. The average of the O^{4+} beam intensity was about 2 enA.

The calculated angular momentum l brought into a compound nucleus was $38\hbar$ according to the Bass model calculation [20]. The beam energy was selected to be 100 MeV according to the results of the calculation made by the statistical-model code CASCADE. The predicted fusion cross-section of about 300 mb is consistent with the experimental result.

For the γ-ray detection, 2 BGO anti-Compton shielded and one unshielded clover-type Ge detectors, 2 co-axial and 1 LEPS Ge detectors were used. The clover detectors were operated in the add-back mode for the γ-γ coincidence measurement and in direct mode for angular-distribution measurement. The relative efficiencies of 2 co-axial–type Ge detectors were 40% and 50%. Two clover-type Ge detectors were located at an angle $\theta = 90^\circ$ with respect to the beam axis and were used for linear-polarization measurements. Two co-axial– and LEPS–type Ge detectors were placed at angles $\theta = 50^\circ$, 158° and 141° with respect to the beam axis. The distances between the target and the surfaces of the Ge detectors were 13 cm.

The total detection efficiency of the γ-ray was 0.73% at 1.3 MeV in the singles mode. A total of 1.2×10^9 coincidence events were recorded in event-by-event mode for off-line analysis. In addition to the coincidence measurement, a beam-delayed two-dimensional measurement, γ-ray energy *versus* time, was performed in order to search for the short-lived isomer. This measurement was performed in parallel with coincidence measurements using another independent data acquisition system.

2.1 Prompt γ-γ coincidences

A level scheme of ^{93}Mo was established in the past up to the 35/2 states at 7.3 MeV [16]. Figure 3 shows the proposed level scheme of ^{93}Mo based on the γ-γ coincidence data. The gate width of prompt γ-γ timing was set to 200 ns. The coincidence relations of known γ-rays agree with those in the previous report except for the 1067 keV transition. A known γ-ray of 1067 keV which was previously reported [16] as a transition populating the $29/2^+$ state at 5585 keV was placed to populate the 35/2 at 7268 keV state based on the present coincidence result.

The ordering of each level was determined considering the intensity balances and the coincidence relations. There were coincidence relations between the 648 keV γ-ray and γ-rays below the 8353 keV state as well as those below the $29/2^+$ state at 5585 keV. However, no transition linking

Table 1. Measured γ-ray energies, intensities, angular-distribution coefficients and linear-polarization values in ^{93}Mo. Relative intensities are normalized to the 1734 keV γ-ray intensity. Uncertainties are given in parentheses.

E_γ (keV)	I_γ	A_2/A_0	Polarization	$E_i \rightarrow E_f$	$J_i \rightarrow J_f$
241.6	43(7)	–0.19(4)		7268 → 7026	$35/2 \rightarrow 33/2$
260.2	doublet[b]			6837 → 7097	
262.4	doublet[b]			8597 → 8335	
263.0				2425 → 2162	$21/2^+ \rightarrow 13/2^+$
278.4	60(5)	0.10(5)	0.15(4)	4437 → 4159	$27/2^- \rightarrow 23/2^-$
476.0	9(3)[a]			9646 → 9170	
573.4	14(5)[a]			9170 → 8597	
647.6	2(1)[a]			9001 → 8353	
668.6	2(1)[a]			9669 → 9001	
684.5				2162 → 1477	$13/2^+ \rightarrow 9/2^+$
685.9	58(4)[a]	0.072(6)	0.06(3)	5585 → 4899	$29/2^+ \rightarrow 25/2^+$
1066.6	10(3)[a]			8335 → 7268	
1147.4	18(2)	–0.37(13)	0.11(6)	5585 → 4437	$29/2^+ \rightarrow 27/2^-$
1441.5	29(2)	0.12(9)	–0.44(14)	7026 → 5585	$33/2^- \rightarrow 29/2^+$
1477.1				1477 → 0	$9/2^+ \rightarrow 5/2^+$
1516.3	2(1)[a]			8353 → 6837	
1552.4	6(2)[a]			8820 → 7268	
1570.7	5(1)			8597 → 7026	
1734.4	100(6)	–0.39(7)	0.023(6)	4159 → 2425	$23/2^- \rightarrow 21/2^+$
2399.4	8(1)			6837 → 4437	
2474.1	57(3)	0.17(8)	0.019(9)	4899 → 2425	$25/2^+ \rightarrow 21/2^+$

([a]) Estimated from coincidence data.
([b]) Unresolved doublet.

the 8353 keV and the 5585 keV levels was observed in this work. The same occurs for a transition between the 9001 keV and the $33/2^-$ states at 7026 keV.

Figure 4 shows background-subtracted γ-ray spectra. Figure 4(a) is the spectrum gated by the 1067 keV γ-ray. Figures 4(b), (c) are the spectra gated by newly found γ-rays and new γ-rays can be seen. The transitions marked by an asterisk in figs. 3 and 4 are new ones. Intensities and placements in the level scheme of all γ-rays observed in this work are given in table 1. The 276 keV transition was not listed because the coincidence relation could not be determined. Gamma-ray intensities given with (a) were obtained from singles data. Those with (b) were deduced using gated spectra.

2.2 Angular distributions

In order to assign spin values of the states, angular-distribution measurements were performed. The spin change, ΔI, of each transition was deduced based on these results. Gamma rays were detected in singles mode by clover-type Ge detectors located at angles 38°, 50°, 76°, 90° and 158°. The singles γ-ray spectra from each Ge crystal in clover detectors were treated independently. The angular-distribution data were fitted to the Legendre polynomial expansion

$$\mathcal{W}(\theta) = \sum A_\nu P_\nu(\cos\theta), \tag{1}$$

where ν's are even numbers. The extracted A_2/A_0 coefficients are listed in table 1.

2.3 Linear polarizations

Linear-polarization measurements are useful in determining the electric or magnetic character of γ-radiation as well as spins of initial and final states. By combining the results of linear-polarization and angular-distribution measurements, information on the multipolarity of γ-radiation as well as spins of the initial and final states and the spin and parity of the concerned nuclear state can be assigned.

These measurements were performed by using a spectrum taken by the clover detectors located at an angle $\theta = 90°$ with respect to the beam axis. The clover detectors act as a polarimeter when the Compton-scattered events give signals in adjacent crystals. The coincidence events were separated according to the condition whether the coincidence events from the adjacent crystals are either from parallel or perpendicular ones to the reaction plane. The linear polarization P is defined by the following equation:

$$P_{\exp} = A/Q, \tag{2}$$

where

$$A = (W_\perp - W_\parallel)/(W_\perp + W_\parallel), \tag{3}$$

$W_\perp$ and $W_\parallel$ denote the perpendicular and the parallel Compton scattering amplitude, respectively. Q represents

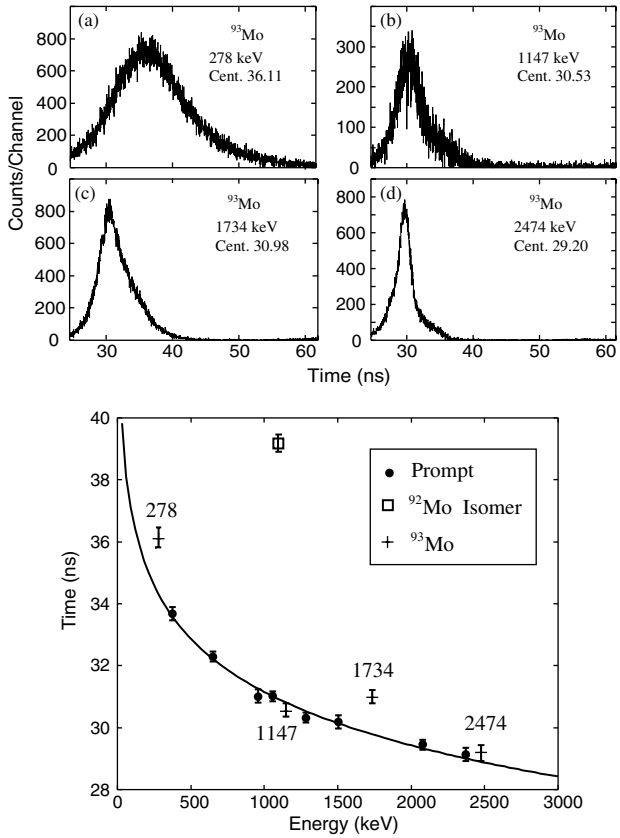

Fig. 5. The examples of the time distribution spectra of γ-ray transitions 278 keV (a), 1147 keV (b), 1734 keV (c) and 2474 keV (d) (top). Time *versus* γ-ray energy plot of extracted centroids (bottom). The prompt γ-rays are represented by the filled circles. The γ-ray from isomeric states in ^{92}Mo and four transitions in ^{93}Mo are denoted by a box and crosses, respectively.

the polarization sensitivity of the polarimeter and is a function of the incident γ-ray energy.

Table 1 shows measured linear-polarization values and transition assignments were made assuming pure multipolarities for γ-rays. The transition multipolarity assignment was based on angular-distribution measurements. Based on these results, spins and parities of 5 states in ^{93}Mo were determined.

2.4 Off-beam γ-rays

To search for the short-lived isomer, a beam delayed two-dimensional measurement, E_γ *versus* time, was performed in parallel with the coincidence measurement. In this measurement, the γ-ray energy spectra were recorded with time information between γ-rays and beam pulses of the cyclotron. These pulses, which were produced by the RF signal, had a spacing of 83 ns. The time distribution measurements allow one to find delayed transitions.

An isomer search using the centroid-shift method was performed. In the lifetime measurement, the usual procedure is to measure a decay curve. However, for a short

Table 2. Observed γ-rays in ^{93}Mo and their intensities obtained in a delayed spectrum. Relative intensities are obtained by normalizing to those of a prompt spectrum.

γ-ray energy (keV)	Area (counts)	Relative intensity
242	doublet with ^{92}Mo	–
278	7701	0.48(3)
686	2106	0.46(13)[a]
1147	1913	0.28(4)
1442	no peak	–
1734	3019	0.60(8)
2474	926	0.22(4)

([a]) The large error is due to the background of the delayed γ-ray from the ^{72}Ge(n, n$'$) reaction.

lifetime compared with the detector time resolution, the centroid-shift method is useful [21]. The examples of time distribution spectra are shown in fig. 5 (top). The centroids of the spectra were evaluated by fitting these spectra. Centroids of prompt γ-rays are plotted in fig. 5 (bottom) by filled circles and the relation between times and γ-ray energies was obtained as the following equation using a least-square fitting:

$$T = 48.3(10) - 2.48(14)\ln(E_\gamma), \quad (4)$$

where T is the centroid of the time spectrum in ns and E_γ is the γ-ray energy in keV.

This fitted prompt curve is also shown in fig. 5 by a solid line. The points of 4 transitions 278, 1147, 1734 and 2474 keV in ^{93}Mo are shown by crosses. The centroids of 278 and 1734 keV transitions are deviated from the curve for the centroids of prompt transitions. On the other hand, centroids of 1147 and 2474 keV transitions are on the curve. This indicates that the $27/2^-$ state at 4437 keV in ^{93}Mo is an isomer The half-life of this isomer obtained by the conventional centroid-shift method based on the 278 and 1735 keV time distribution spectra was 0.8±0.2 ns. The square in fig. 5 shows a γ-ray de-exciting a known isomer in ^{92}Mo. The half-life of this isomer was taken to be 8.2(8) ns, which is consistent with the value previously reported [22].

2.5 Delayed γ-γ coincidences

To search for a relatively long-lived isomer, a γ-γ delayed-coincidence analysis was carried out. The event data used in this analysis were the same as those used in a prompt coincidence analysis. Figure 6 shows a delayed γ-γ projection spectrum. This spectrum was made by subtracting a pre-prompt spectrum from a post-prompt one. The delayed time conditions of these two spectra were set in ranges of 1 to 3 μs on both sides of the prompt peak.

Delayed γ-rays from several nuclei which have isomeric states were observed as positive peak. The transition energies and lifetimes of these isomers are indicated in the

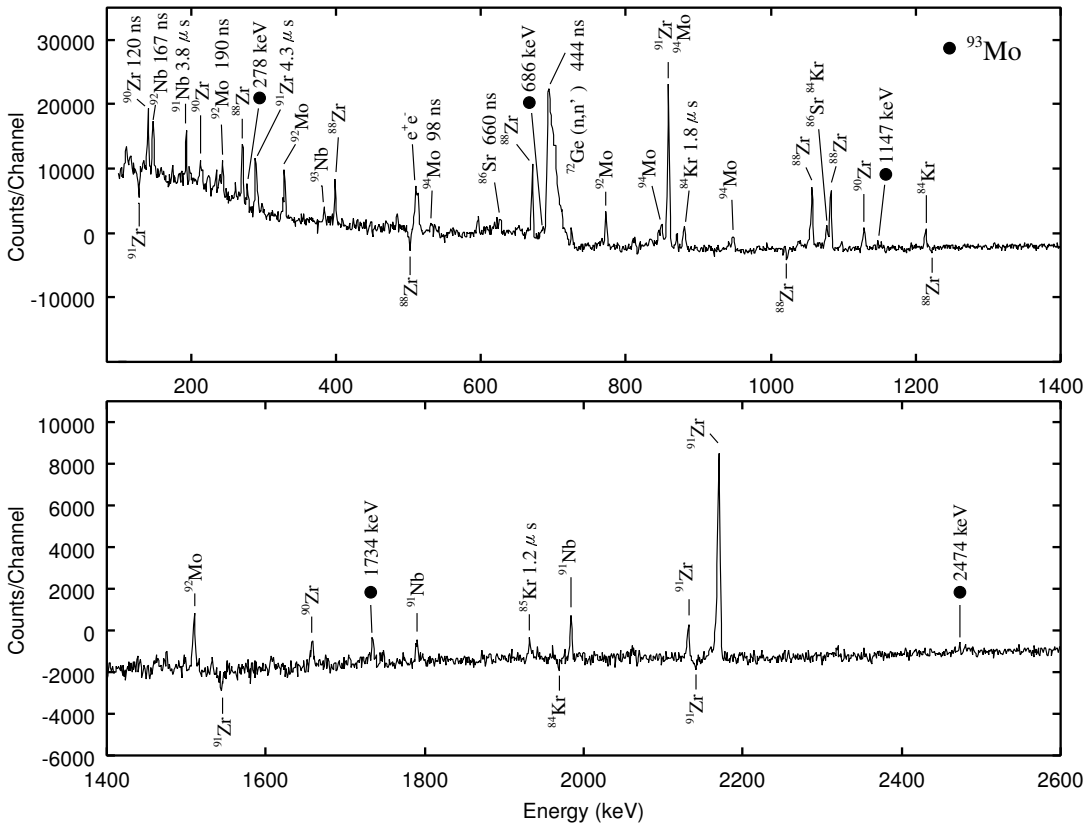

Fig. 6. Spectrum obtained from the difference between a post-prompt spectrum and a pre-prompt one.

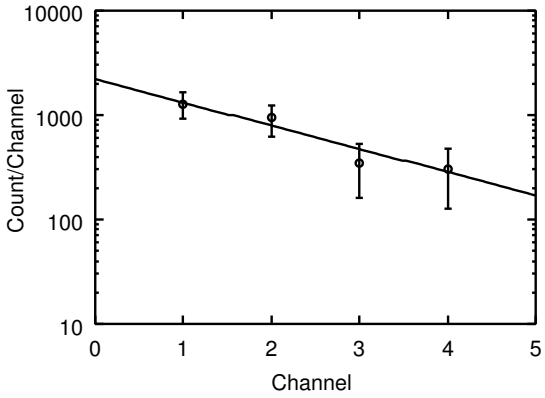

Fig. 7. Time distribution of 1734 keV which reflects the lifetime of the isomer in ^{93}Mo. One channel corresponds to 10 RF bunchs (830 ns).

spectrum. In this spectrum, several γ-rays in ^{93}Mo were observed. The observation of γ-rays of ^{93}Mo indicates the existence of a relatively long-lived isomer. Observed delayed γ-ray energies and intensities of ^{93}Mo are given in table 2. Based on the intensities of each cascade, a high-spin isomer was located above the 669 keV γ-ray transition.

Figure 7 shows the time distribution of a 1734 keV γ-ray in a cascade de-exciting the high-spin isomer at about 9.7 MeV in ^{93}Mo. From this spectrum, the half-life of the high-spin isomer was determined to be $T_{1/2} = 1.1^{+1.5}_{-0.4}$ μs. By using the lifetime information, the population of this high-spin isomer is taken to be $1.8^{+1.0}_{-1.5}$%.

Table 3. Measured γ-ray energies, intensities, angular-distribution coefficients and linear-polarization values in ^{92}Mo.

E_γ (keV)	I_γ	$E_i \rightarrow E_f$	$J_i \rightarrow J_f$
84.6		2611.7 → 2526.8	$6^+ \rightarrow 5^-$
110.4	11(3)	6659.9 → 6549.5	$13^- \rightarrow 12^-$
147.1	45(6)	2758.8 → 2611.7	$8^+ \rightarrow 6^+$
234.7	26(5)	4484.8 → 4250.6	$11^- \rightarrow 9^-$
244.2	57(6)	2526.8 → 2282.6	$5^- \rightarrow 4^+$
329.1	55(5)	2611.7 → 2282.6	$6^+ \rightarrow 4^+$
536.4	10(3)	8920.5 → 8384.1	$16^- \rightarrow 15^-$
557.1	13(3)	9477.6 → 8920.5	$17^- \rightarrow 16^-$
626.5	31(5)	4250.6 → 3624.1	$9^- \rightarrow 7^-$
649.7	37(5)	7309.6 → 6659.9	$14^- \rightarrow 13^-$
739.4	14(3)	5859.5 → 5119.7	$12^+ \rightarrow 10^+$
772.8	96(5)	2282.6 → 1509.8	$4^+ \rightarrow 2^+$
800.1	13(3)	6659.9 → 5859.5	$13^- \rightarrow 12^+$
1074.5	18(3)	8384.1 → 7309.6	$15^- \rightarrow 14^-$
1097.3	33(6)	3624.1 → 2526.8	$7^- \rightarrow 5^-$
1374.7	5(2)	5859.5 → 4484.8	$12^+ \rightarrow 11^-$
1509.8	100(5)	1509.8 → 0	$2^+ \rightarrow 0^+$
2064.7	37(5)	6549.5 → 4484.8	$12^- \rightarrow 11^-$
2360.9	16(3)	5119.7 → 2758.8	$10^+ \rightarrow 8^+$

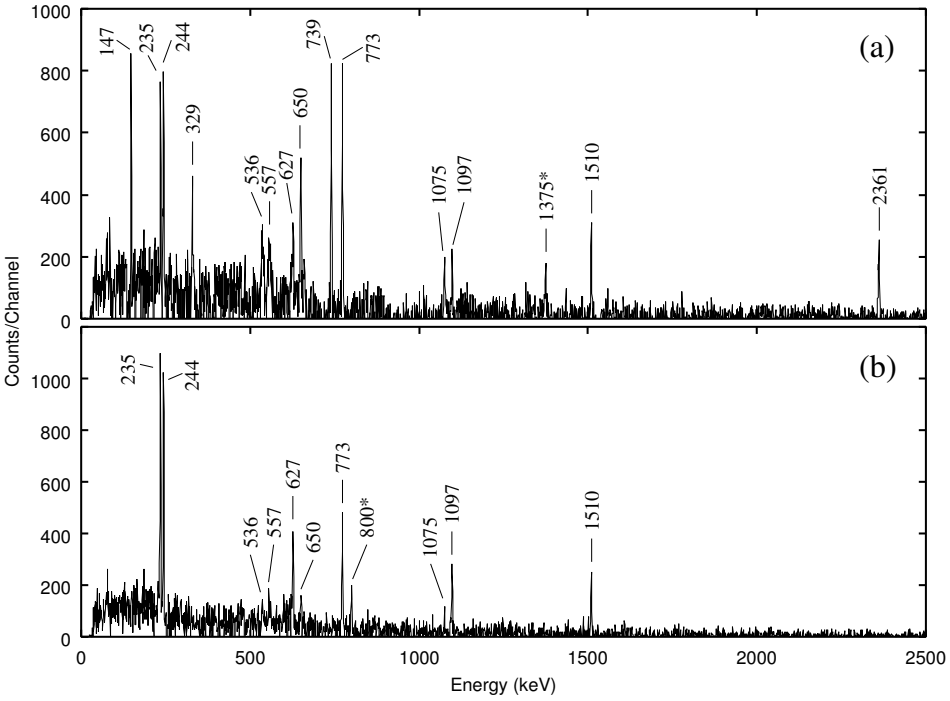

Fig. 8. Spectra obtained by gating on 1375 keV (a) and 800 keV (b) γ-rays, respectively.

2.6 Level scheme of ^{93}Mo

Figure 3 shows the proposed level scheme of ^{93}Mo. The transitions marked by an asterisk are new ones. The widths of the arrows indicate γ-ray intensities. A level scheme was extended up to the states at 9.7 MeV based on the coincidence relations and γ-ray intensities. Ten new γ-rays and 10 new levels were newly identified. Spins and parities of 5 levels were assigned. The spin changes, ΔI, of transitions were deduced based on angular-distribution measurements. The spin assignments of each level were given by considering both ΔI values and γ-ray cascade crossover relations.

Two isomeric states were newly found using beam-delayed and delayed γ-γ coincidence analysis. An isomer of the $27/2^-$ state is located at 4.4 MeV excitation energy with a 0.8 ns half-life. The excitation energy of another high-spin isomer is about 9.7 MeV. This might be the expected $(39/2^-)$ isomer. The tentative spin and parity assignments of the high-spin isomer at 9.7 MeV were made based on a configuration of the high-spin isomer discussed in sect. 1. A high-spin isomer was found observing γ-rays de-exciting the states up to 9669 keV. Assuming dipole and/or quadrupole characters for transitions as well as the postulated low-energy transition between the isomer and the 9669 keV level, the spin and parity of the isomer could be $39/2^-$ as a consequence of the $1\hbar$ increase for each transition.

A low-energy transition x which de-excites the high-spin isomer was tentatively placed above the 669 keV γ transition. Because the γ-ray x was expected to be of low energy and weak transition, this γ-ray was unobserved. The diagram on the right of fig. 3 shows the intensity of the

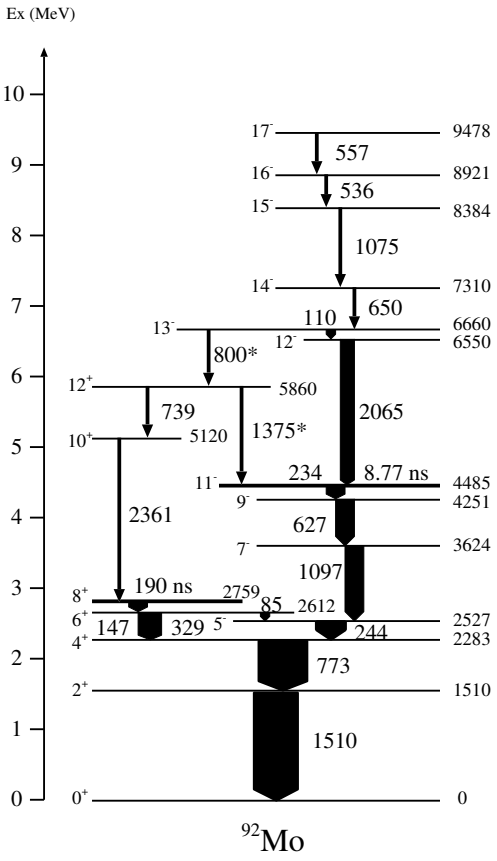

Fig. 9. The proposed level scheme for ^{92}Mo. The width of the arrows indicates γ-ray intensities, while the energy is indicated in units of keV. The marked transitions by asterisk are new ones.

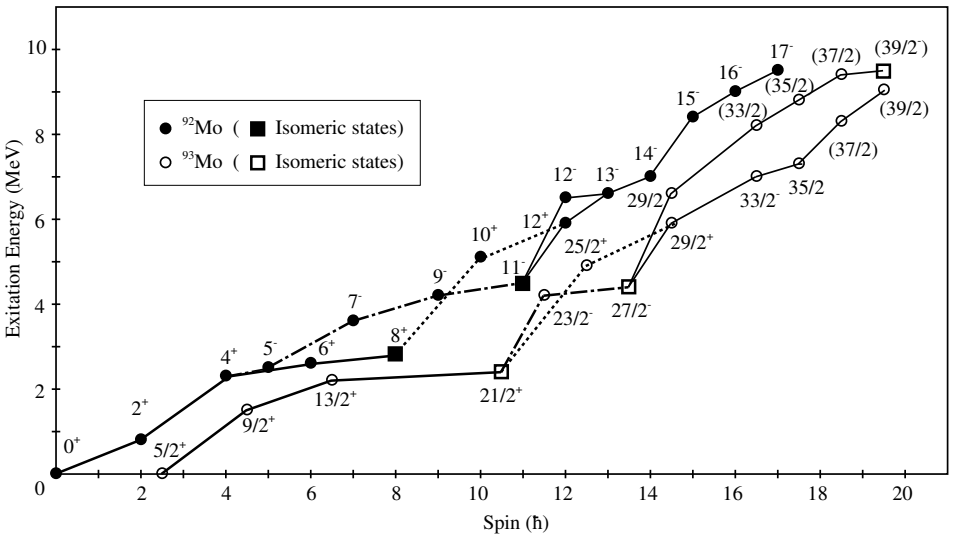

Fig. 10. The yrast lines of ^{92}Mo and ^{93}Mo. States in ^{92}Mo and ^{93}Mo are indicated by closed and opened circles, respectively. The isomeric states are indicated by squares.

feeding γ-rays at each level. Since above the 5.6 MeV excitation energy, the intensity balances of γ-rays do not hold and are weaker than those below 5.6 MeV states, many unobserved weak and high-energy γ-rays seem to exist.

2.7 Level scheme of ^{92}Mo

In order to compare the level structures of ^{93}Mo and ^{92}Mo, a level scheme of ^{92}Mo was also constructed in the present work using the prompt-coincidence method. ^{92}Mo was populated as a by-product of ^{93}Mo via the reaction ^{82}Se(^{16}O, 6n) ^{92}Mo. The results are listed in table 3. Two γ transitions linking positive- and negative-parity states were newly found in this work. Figure 8 shows γ-ray spectra obtained by gating on newly found γ-rays of ^{92}Mo. Figure 9 shows the proposed level scheme of ^{92}Mo. The transitions marked by an asterisk are new ones.

3 Discussion

The high-spin states of ^{93}Mo, one of the $N = 51$ isotones, were studied. They are expected to have similar characteristics to those of the $N = 83$ isotones [1–8] because of the similarity of shell model orbits near the Fermi level including proton sub-shell closures of $Z = 40$, 64 and neutron shell closures of $N = 50$, 82 as shown in fig. 1. As was pointed out in sect. 1, in $N = 51$ odd-mass isotones, there are $21/2^+$ isomers of a $[\nu(d_{5/2})\otimes\pi(g^2_{9/2})]$ configuration which are analogous to $27/2^-$ isomers of a $[\nu(f_{7/2})\otimes\pi(h^2_{11/2})]$ configuration in $N = 83$ odd-mass isotones.

There are three isomeric states in ^{93}Mo and two of them were found in this work. An isomer at $21/2^+$ which has the above-mentioned configuration with the lowest excitation energy of the three was previously reported [16].

A new isomer of $27/2^-$ with a half-life of 0.8 ns was found in ^{93}Mo. This state may be interpreted to stem from the weak coupling of $\nu(d_{5/2})$ to the 11^- isomer of ^{92}Mo based on their excitation energies and the energy spacings of the next lower excited states. This half-life is 16 times shorter than that of its Weisskopf estimate. This enhancement of an $E2$ transition rate is much larger compared with that of the 11^- isomer of ^{92}Mo which is enhanced by a factor 3.5. This may indicate that the $27/2^-$ state of ^{93}Mo consists of many configurations in addition to the $\nu(d_{5/2})\otimes 11^-$ states leading to a larger collectivity to the states in ^{93}Mo.

The weak-coupling feature of the states of ^{93}Mo resulted from a coupling of $\nu(d_{5/2})$ to those of ^{92}Mo may be seen in fig. 10. Their excitation energies of the states in ^{93}Mo and ^{92}Mo are plotted as a function of spin. Similar behaviors are seen for those of both nuclei. This fact supports the interpretation that the yrast and near-yrast states in ^{93}Mo result from the weak coupling of $\nu(d_{5/2})$ to states in ^{92}Mo.

Using the above-mentioned tentative spin assignments, an yrast state of spin 35/2 is the 7268 keV state as shown in fig. 10. When the yrast states are extended assuming quadrupole transitions for the 1570 keV transition and a dipole transition for the 573 keV transition, the high-spin isomer of ^{93}Mo is not an yrast state. This non-yrast feature of the isomer may be consistent with the small population of the isomer, namely about 2% of the population of the total production of ^{93}Mo. If this high-spin isomer is a shape isomer as same as those of $N = 83$ isotones, the high hindrance of its decay to yrast states can be explained. The small population of the high-spin isomer, in case of $N = 51$ isotones, is very much different from the feature observed in $N = 83$ isotones.

4 Summary

A new high-spin isomer of $(39/2^-)$ was found in ^{93}Mo. This isomer has probably the same kind of structure as

that of high-spin isomers in $N = 83$ isotones, namely the stretch coupling of angular momenta of the valence nucleons along the symmetry axis. The high-spin isomer of this kind was found, for the first time in $N = 51$ isotones. The non-yrast character of this isomer is unique in comparison with those of $N = 83$ isotones. Another new isomer of $27/2^-$ may be understood as a state resulted mainly from the weak coupling of $\nu(d_{5/2})$ to the 11^- isomer of ^{92}Mo. However, the measured half-life shows much enhancement in comparison with that of the 11^- isomer of ^{92}Mo indicating larger collectivity of the new $27/2^-$ isomer.

This work was supported by the Department of Physics, Kyushu University. We wish to thank all staffs at Cyclotron and Radioisotopes Center (CYRIC) in Tohoku University.

References

1. X.H. Zhou *et al.*, Phys. Rev. C **61**, 014303 (1993).
2. T. Murakami *et al.*, Z. Phys. A **345**, 123 (1993).
3. A. Odahara *et al.*, Nucl. Phys. A **620**, 363 (1997).
4. E. Ideguchi *et al.*, Z. Phys. A **352**, 363 (1995).
5. R. Broda *et al.*, Z. Phys. A **305**, 281 (1982); O. Bakabder *et al.*, Nucl. Phys. A **389**, 93 (1982).
6. Y.H. Zhang *et al.*, High Energy Phys. Nucl. Phys. **20**, 20 (1996).
7. M. Gupta *et al.*, Phys. Rev. C **54**, 1610 (1996).
8. Y. Gono *et al.*, to be published.
9. S. André *et al.*, Z. Phys. A **337**, 349 (1990); C. Foin *et al.*, Eur. Phys. J. A **8**, 451 (2000).
10. T. Døssing *et al.*, Phys. Scr. **24**, 258 (1981).
11. O. Häusser *et al.*, Nucl. Phys. A **379**, 287 (1982).
12. O. Häusser *et al.*, Phys. Rev. Lett. **42**, 1451 (1979); E. Dafni *et al.*, Nucl. Phys. A **443**, 135 (1985).
13. E.K. Warburton *et al.*, J. Phys. G **12**, 1017 (1986).
14. B.A. Brown *et al.*, Phys. Rev. C **13**, 1900 (1976).
15. B.A. Brown *et al.*, Phys. Rev. C **15**, 2044 (1977).
16. A.E. Zobov *et al.*, Nucl. Data. Sheets **80**, 1 (1997).
17. I.Y. Lee *et al.*, Phys. Rev. C **24**, 293 (1981).
18. P. Chowdhury *et al.*, Phys. Rev. C **32**, 1238 (1985).
19. W.F. Piel *et al.*, Phys. Rev. C **41**, 1223 (1990).
20. R. Bass, Phys. Lett. B **47**, 139 (1973).
21. R.S. Weaver, R.E. Bell, Nucl. Instrum. Methods **9**, 149 (1960); W. Andrejtscheff *et al.*, Nucl. Instrum. Methods **204**, 123 (1982).
22. P. Singh *et al.*, Phys. Rev. C **45**, 45 (1992).
23. B. Crowell *et al.*, Phys. Rev. Lett. **72**, 1164 (1994) and references therein.